 DOI: https://doi.org/10.5114/ceji/220659

Puerarin alleviates oxidative stress-induced mitochondrial dysfunction in human lens epithelial cells through modulation of *DLG1* expression

SHAOXIN PAN[*], *WEI LI*[*], *DANDAN SU*

Ophthalmology Medical Center, The Second Affiliated Hospital of Wannan Medical College, Wuhu, Anhui Province, 241000, People's Republic of China

[*]These authors contributed equally to this study.

Abstract

Introduction: *Oxidative stress and mitochondrial dysfunction are key contributors to age-related cataract (ARC) development. This study investigated the role of DLG1 in oxidative injury in human lens epithelial cells (HLECs) and whether puerarin (Pue) could alleviate oxidative stress and mitochondrial dysfunction.*

Material and methods: *Gene co-expression networks were constructed for differentially expressed genes (DEGs) in GSE3040 along with GSE213546. Expression, diagnostic performance, and enrichment analyses were performed on the overlapping genes in the two datasets. Functional assays were performed in hydrogen peroxide (H_2O_2)-induced HLECs to evaluate the role of DLG1 and Pue's impact on oxidative stress and mitochondrial function.*

Results: *DLG1, histone H4 (HIST1H4L), N alpha acetyltransferase 16 (NAA16), and Scratch family transcriptional repressor 1 (SCRT1) were consistently upregulated in ARC and exhibited high diagnostic performance. In HLECs, H_2O_2 increased the mRNA levels of all four genes, whereas co-treatment with Pue reversed these changes. Functionally, small interfering RNA (siRNA)-mediated DLG1 silencing mitigated oxidative stress-induced cell injury, while DLG1 overexpression produced the opposite effect. Molecular docking indicated a favorable Pue–DLG1 binding affinity. Pue significantly attenuated H_2O_2-induced decreases in cell viability, mitochondrial membrane potential, and increased mitochondrial reactive oxygen species (ROS). Notably, DLG1 overexpression attenuated the protective effects of Pue against oxidative damage and mitochondrial dysfunction.*

Conclusions: *DLG1 plays a pro-damage role in oxidative stress-induced HLEC damage, while Pue exerts a protective effect partly through modulation of DLG1 expression. These findings suggest that DLG1 may serve as a potential target for ARC, with Pue representing a potential intervention candidate.*

Key words: *age-related cataracts, puerarin, DLG1, oxidative stress, mitochondrial dysfunction, human lens epithelial cells.*

(Cent Eur J Immunol 2026; 51 (3): 1-17)

Introduction

The most frequent kind of cataract is age-related cataract (ARC) [1], with its development influenced by multiple factors including oxidative stress, metabolic disorders, genetic predisposition, environmental exposures, and lifestyle habits [2, 3]. Multiple studies have shown that oxidative stress is a key driver in ARC onset and progression [4, 5]. Under normal circumstances, the antioxidant system of the lens can eliminate excess reactive oxygen species (ROS), thereby protecting the lens from oxidative damage and maintaining its transparency [6]. However, with aging, this antioxidant capacity gradually declines, leading to a decrease in glutathione (GSH) reserves and increased protein oxidation and aggregation, ultimately impairing lens structure and function [7]. In lens epithelial cells, mitochondria are the main ROS source, and aging or oxidative stress can disrupt the electron transport chain, causing electron leakage and ROS overproduction [8]. Excess ROS aggravates

Correspondence: Shaoxin Pan, Ophthalmology Medical Center, The Second Affiliated Hospital of Wannan Medical College, No. 10, Kangfu Road, Jinghu District, Wuhu city, Wuhu, Anhui Province, 241000, People's Republic of China, e-mail: 13965880135@163.com
Submitted: 08.11.2025, Accepted: 14.04.2026

mitochondrial damage, creating a vicious cycle that drives protein aggregation, lens opacity, and ARC progression [9]. Thus, interventions targeting this process may provide new insights into the prevention and treatment of ARC.

Discs large MAGUK scaffold protein 1 (DLG1) is a multidomain scaffold protein involved in maintaining cell polarity and neuronal function, as well as the development and progression of related diseases [10, 11]. For example, knocking out *DLG1* expression inhibits microglial activation and alleviates lipopolysaccharide-induced depressive-like behavior in mice [12]. Supporting this conclusion, another study showed that the loss of *DLG1* in microglia ameliorates depressive-like behavior induced by chronic restraint stress by reducing the number of activated microglia and reversing their morphological changes [13]. Another study demonstrated that *DLG1* enhances antiviral innate immune responses by inhibiting p62-mediated autophagic degradation of iκB kinase epsilon (IKKε) [14]. However, its potential role in the pathogenesis of ARC remains unclear.

Puerarin (Pue) is an isoflavone derivative extracted from the traditional Chinese medicine Pueraria lobata [15, 16]. It has been shown to enhance blood circulation, reduce blood stasis, improve microcirculation, dilate coronary and cerebral arteries, and decrease myocardial oxygen consumption [17, 18]. Clinically, Pue injections are also used to treat cardiovascular and cerebrovascular diseases, retinal vascular issues, fundus conditions, and sudden deafness [19, 20]. Recently, some research has been concentrated on the molecular mechanisms of Pue activity. Literature reports suggest that Pue can regulate signaling pathways such as nuclear factor kappa-light-chain-enhancer of activated B cells (NF-κB), mitogen-activated protein kinases (MAPKs), and phosphoinositide 3-kinase/protein kinase B (PI3K/AKT), influencing the expression of inflammatory factors, thereby exerting anti-inflammatory, antioxidant, as well as anti-apoptotic effects in diseases [21-24]. Additionally, Pue eye drops can lower intraocular pressure by blocking β-receptors and are used clinically to treat ocular hypertension and glaucoma [25]. However, the role of Pue in cataracts and oxidative stress in lens epithelial cells remains unclear. Therefore, exploring the antioxidant and protective mechanisms of Pue in lens epithelial cells is vital for understanding its potential in preventing and treating ARC.

Based on high-throughput transcriptome data, combined with bioinformatics methods such as weighted gene co-expression network analysis (WGCNA), this study screened key regulatory genes associated with ARC and identified *DLG1* as a hub gene. The role of *DLG1* in oxidative stress-induced damage in human lens epithelial cells (HLECs) and whether Pue affects DLG1, cell survival, and mitochondrial activity in this process were examined using an *in vitro* model. By elucidating the function of DLG1 in ARC pathogenesis and its interaction with Pue, this study is expected to provide potential molecular targets and drug candidates for targeted intervention of ARC.

Material and methods

Searching for ARC-related datasets

Transcriptome datasets (GSE3040, GSE213546) were obtained from the Gene Expression Omnibus (GEO) database (https://www.ncbi.nlm.nih.gov/geo/). GSE3040 was generated on the GPL96 [HG-U133A] Affymetrix Human Genome U133A array and includes 12 HLE B-3 lens epithelial cell samples treated with vehicle or dexamethasone (DEX) for 4 or 16 h [26]. GSE213546 was generated on the GPL10558 Illumina HumanHT-12 V4.0 platform and contains six anterior lens capsule samples from human donors (three ARC and three normal). Normalized data were analyzed using "limma" (version 3.42.2) in R to identify differentially expressed genes (DEGs), with thresholds of fold change (FC) > 1.5 or FC < 0.67 and $p < 0.05$.

Construction of gene co-expression network and module-trait correlation analysis

To explore gene co-expression patterns and identify cataract-related modules, WGCNA was performed on DEGs identified from the GSE3040 and GSE213546 datasets using the "WGCNA" package (version 1.71) in R software. First, a sample cluster dendrogram was generated to assess outliers. The adjacency matrix was constructed using a soft-threshold power that met the scale-free topology condition, and it was then translated into a topological overlap matrix (TOM). Gene clustering was performed using average linkage, and modules were detected via dynamic tree cutting. Module eigengenes (MEs) were then associated with clinical characteristics (cases and controls) to identify modules most relevant to the disease phenotype.

Identification, diagnostic evaluation, and functional annotation of candidate genes

The Bioinformatics platform (https://www.bioinformatics.com.cn/) was applied to screen and identify intersection genes from the key modules of the GSE3040 and GSE213546 datasets. Subsequently, the "pheatmap" package (version 1.0.12) was used to visualize the expression patterns of these intersection genes across both datasets. Receiver operating characteristic (ROC) curve analysis was then performed using the R package "pROC" (version 1.18.0) to assess the diagnostic performance of these overlapping genes in two datasets. For functional enrichment analysis, Gene Ontology (GO) analysis was performed using the Enrichr website (https://maayanlab.cloud/Enrichr/) to explore the potential roles of candidate

genes in the biological process (BP), cellular component (CC), and molecular function (MF) categories.

HLECs culture and H2O2-induced oxidative stress model

Cell Research (Shanghai, China; cat. no. 6550) provided the HLECs. The cells were grown in Epithelial Cell media (EpiCM, cat. no. 4101), which was made up of 500 ml of baseline media, 10 ml of fetal bovine serum (FBS) (cat. no. 0010), 5 ml of epithelial cell growth supplement (EpiCGS, cat. no. 4152), and 5 ml of Penicillin-Streptomycin (cat. no. 0503). All cells were kept in a humid incubator with 5% CO_2 at 37°C. To mimic oxidative stress conditions associated with ARC *in vitro*, HLECs were exposed to hydrogen peroxide (H_2O_2) at a concentration of 200 μM [27].

Transfection and drug treatment

Following the manufacturer's instructions, model cells were transfected with small interfering RNAs (siRNAs) targeting *DLG1* (si-*DLG1*-1/2/3) using Lipofectamine RNAiMAX (Thermo Fisher, USA) for siRNA transfection or with a *DLG1* overexpression plasmid using Lipofectamine 3000 (Invitrogen, USA) for plasmid transfection. The siRNAs targeting *DLG1* and the overexpression plasmid encoding *DLG1* (*DLG1*-OE) were constructed by GenePharma (Shanghai, China). Pue (50 μM, Pue; MCE, cat. no. HY-N0145R), a compound reported to exert protective effects in ocular diseases, was applied to cells [16], which were harvested 24 hours later for subsequent analyses.

Analysis of molecular docking

The 3D structure of human DLG1 was retrieved from the Protein Data Bank (https://www.rcsb.org/), and the chemical structure of puerarin was obtained from the PubChem database (https://pubchem.ncbi.nlm.nih.gov/). Molecular docking between puerarin and DLG1 was conducted using AutoDock Vina (version 1.1.2) after preprocessing the ligand and protein structures with AutoDockTools (version 1.5.7), including hydrogen addition, charge assignment, and PDBQT format conversion. The docking grid covered the predicted active pocket of DLG1, and results were visualized in PyMOL (version 2.4), with DLG1 shown in green and puerarin in orange.

Quantitative real-time polymerase chain reaction (qRT-PCR)

Following the manufacturer's instructions, TRIzol reagent (Invitrogen, USA) was used to extract total RNA from HLECs. A NanoDrop 2000 instrument (Thermo Fisher, USA) was used to measure the concentration and purity of the RNA. The PrimeScript RT Kit with gDNA Eraser (Takara, Japan) was used to reverse-transcribe one microgram of total RNA into cDNA. Next, using TB Green Premix Ex Taq II (Takara) on a QuantStudio 5 machine (Applied Biosystems, USA), qRT-PCR was carried out. Gene mRNA levels were quantified by qRT-PCR using the $2^{-\Delta\Delta Ct}$ method after normalization to β-actin [28]. Primer sequences for all targets are presented in Table 1.

Western blot

Proteins were extracted from HLECs using radioimmunoprecipitation assay (RIPA) buffer (Beyotime, China) with protease/phosphatase inhibitors (Thermo Fisher, USA). Lysates were cleared by centrifugation at 12,000 ×g for 15 min at 4°C, and protein concentrations were determined with the Pierce bicinchoninic acid (BCA) assay (Thermo Fisher, USA). Equal amounts of protein were denatured at 95°C for 5 min, separated by 10% sodium dodecyl sulfate-polyacrylamide gel electrophoresis (SDS-PAGE), and transferred to polyvinylidene difluoride (PVDF) membranes. After blocking with 5% non-fat milk in Tris-buffered saline with Tween 20 (TBST) for 1 h, membranes were incubated overnight at 4°C with anti-DLG1 (1 : 1000, ab300481, Abcam) or anti-β-actin (1 : 5000, ab8226, Abcam), followed by horseradish peroxidase (HRP)-conjugated secondary antibodies (1 : 5000, Abcam) for 1 h at room temperature. Protein bands were visualized by ECL (Thermo Fisher, USA) and quantified using ImageJ (version 1.8.0), normalized to β-actin.

Cell viability assay

Cell viability was measured with the Cell Counting Kit-8 (CCK-8) kit (Dojindo, Japan) following the supplier's protocol. Briefly, cells (5×10^3/well) were plated in 96-well plates and cultured overnight. After adding 10 μl of CCK-8 solution to 100 μl of medium in each well, the mixture was incubated for two hours at 37°C. Absorbance

Table 1. Primer sequences for candidate genes

Gene	Forward primer (5′-3′)	Reverse primer (5′-3′)
DLG1	CTGCTGAGTGAGGTTGAGGG	CTTCCGGACCGGCATTTTTC
HISTAH4L	TATACGAGGAGACACGCGGA	GGCCTTTGAGGAACCGTGTA
NAA16	TGGACAGTATTCTTTGGCTTTGG	CAGGGTGCCCTAGAACTTGT
SCRT1	GGAATCATGCCCAGGTCCTT	GGCGTCGCCATCGTAGAC
β-actin	TCGTGCGTGACATTAAGGAG	ATGCCAGGGTACATGGTGGT

was then measured at 450 nm using a microplate reader (BioTek, USA).

MitoSOX staining

The MitoSOX Red mitochondrial superoxide indicator (Invitrogen, USA) was used to measure the levels of mitochondrial reactive oxygen species (mtROS) in accordance with the directions provided by the supplier. Following the recommended treatment, cells cultured on glass coverslips in 24-well plates were incubated for 10 minutes at 37°C in the dark with 5 μM MitoSOX Red reagent diluted in HBSS that had been warmed beforehand. Cell nuclei were counterstained with Hoechst 33342 (5 μg/ml; cat. no. C1022; Beyotime, China) following three HBSS washes. A Leica DMi8 microscope (Germany) was used to capture fluorescence images.

JC-1 staining for measurement of mitochondrial membrane potential (MMP)

Mitochondrial membrane potential (MMP) was measured using the JC-1 Mitochondrial Membrane Potential Assay Kit (cat. no. C2006; Beyotime, China) according to the manufacturer's instructions. After treatment, cells on coverslips were incubated with JC-1 at 37°C for 20 min in the dark, rinsed twice with JC-1 buffer, and counterstained with Hoechst 33342 (5 μg/ml; Beyotime, China). Fluorescence images were captured using a Leica DMi8 microscope (Germany).

Statistical analysis

Data were collected from three biologically independent replicates, and data are expressed as mean ± standard deviation (SD). Data normality was assessed using the Shapiro-Wilk test, and sphericity was evaluated with Mauchly's test where applicable. Statistical analyses were conducted using GraphPad Prism 9.0 and R 4.1.0. Group differences were evaluated by unpaired two-tailed Student's *t*-test or one-way analysis of variance (ANOVA) with Tukey's post hoc test. Values of $p < 0.05$ were considered significant.

Results

Identification and enrichment analysis of DEGs in the ARC dataset

GSE3040 revealed 928 upregulated and 22 downregulated genes, while GSE213546 showed 351 upregulated and 369 downregulated genes (Supplementary Fig. 1A, B). WGCNA was then performed on the DEGs of the two datasets, identifying blue and yellow as key modules in GSE3040 as well as blue and turquoise as key modules in GSE213546 (Fig. 1A-D). Cross-analysis of the key modules in the two datasets revealed 15 overlapping genes (Supplementary Fig. 2A). GO analysis of these overlapping genes revealed that in terms of biological processes, they were mainly involved in inflammatory responses and host defense mechanisms, including responses to

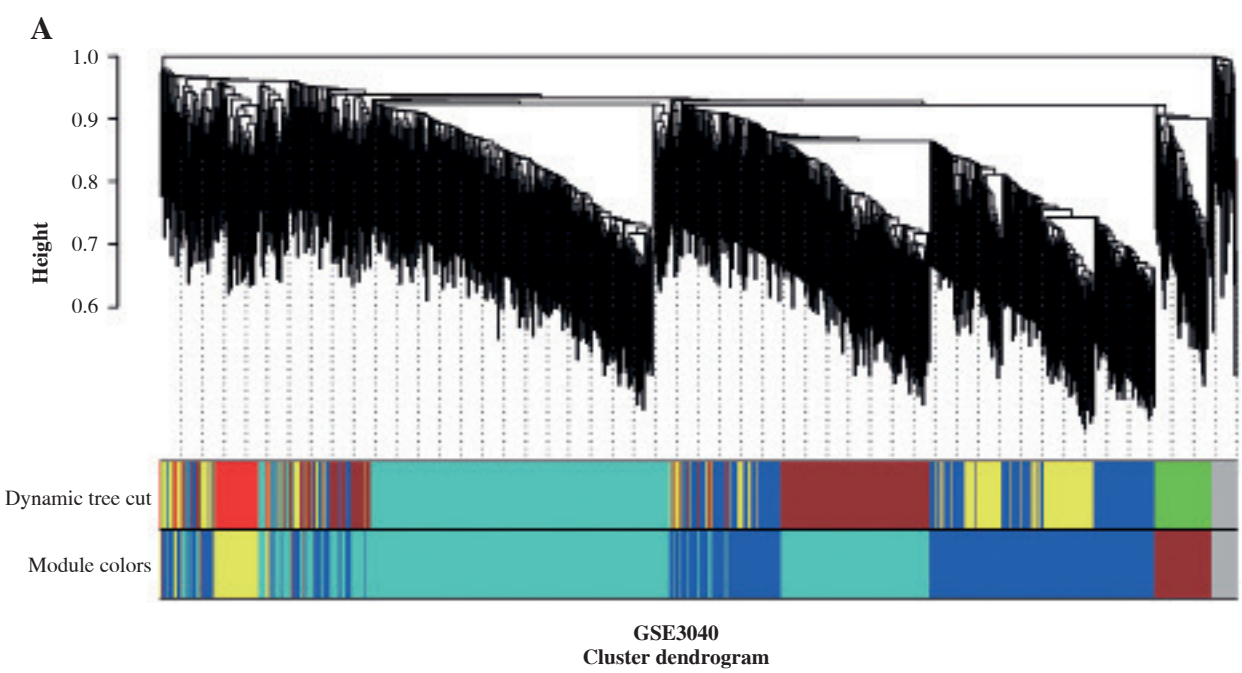

Fig. 1. Weighted gene co-expression network analysis (WGCNA) of differentially expressed genes (DEGs) in age-related cataract (ARC)-related datasets. **A**, **B**) Cluster dendrogram of genes in the GSE3040 (**A**) datasets.

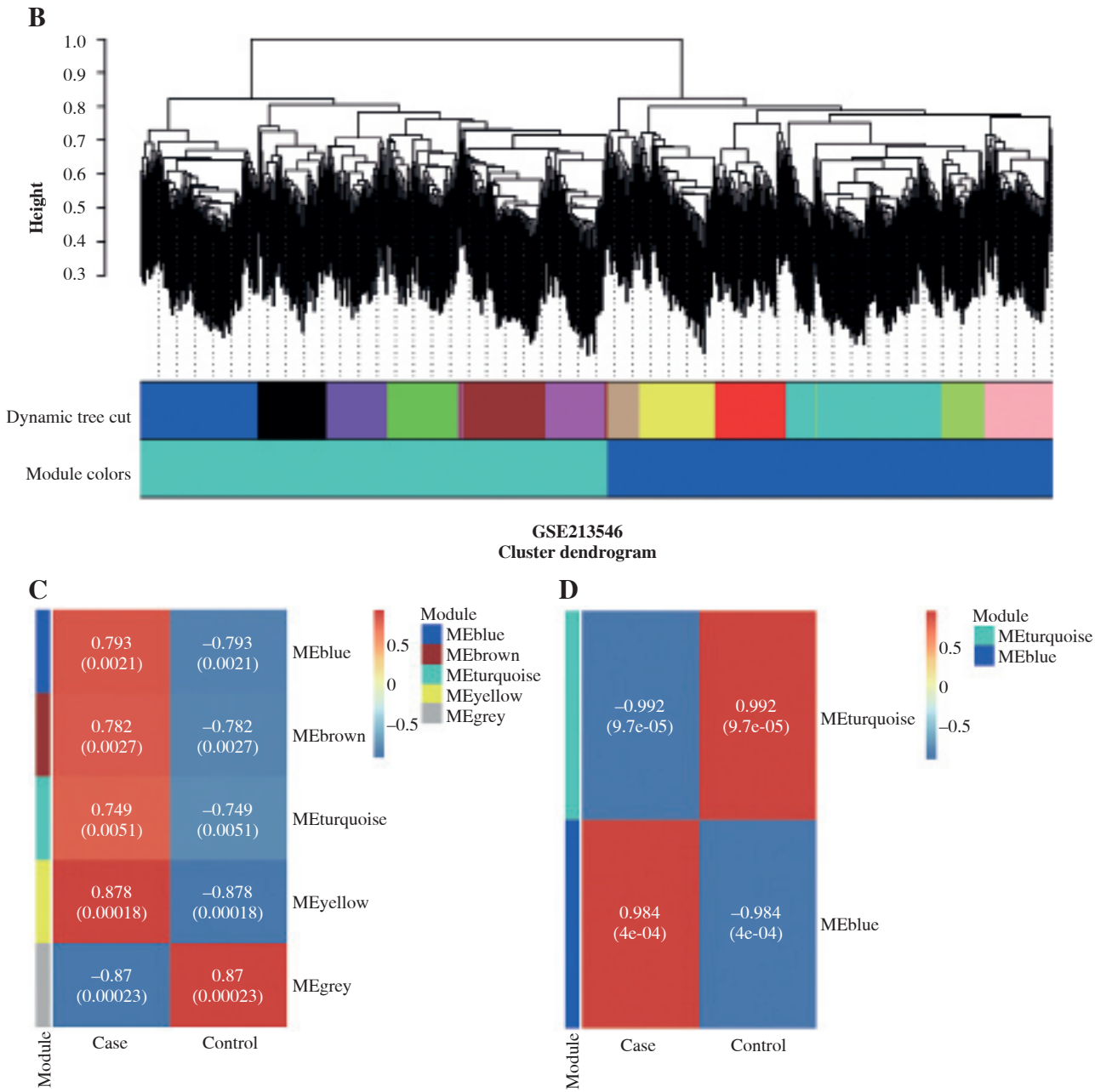

Fig. 1. Cont. **B**) Cluster dendrogram of genes in the GSE213546 (**B**) datasets. Modules were identified using dynamic tree cutting, with each color representing a distinct module. **C**, **D**) Module-trait relationships in the GSE3040 (**C**) and GSE213546 (**D**) datasets. Each cell displays the correlation coefficient between the module eigengene and the clinical trait (case or control), with the corresponding *p* value shown in parentheses. Red indicates a positive correlation, while blue indicates a negative correlation

molecules of bacterial origin (GO: 0002237), neutrophil chemotaxis (GO: 0030593), and cellular responses to interleukin-1 (GO: 0071347) (Supplementary Fig. 2B). Molecular function terms were dominated by calcium ion binding (GO: 0005509), metal ion binding (GO: 0046872), arachidonic acid binding (GO: 0050544), RAGE receptor binding (GO: 0050786), and histone H3 kinase activity (GO: 0140996) (Supplementary Fig. 2C). Cellular component enrichment pointed to cell-cell junction (GO: 0005911), adherens junction (GO: 0005912), desmosome (GO: 0030057), gap junction (GO: 0005921), and others (Supplementary Fig. 2D).

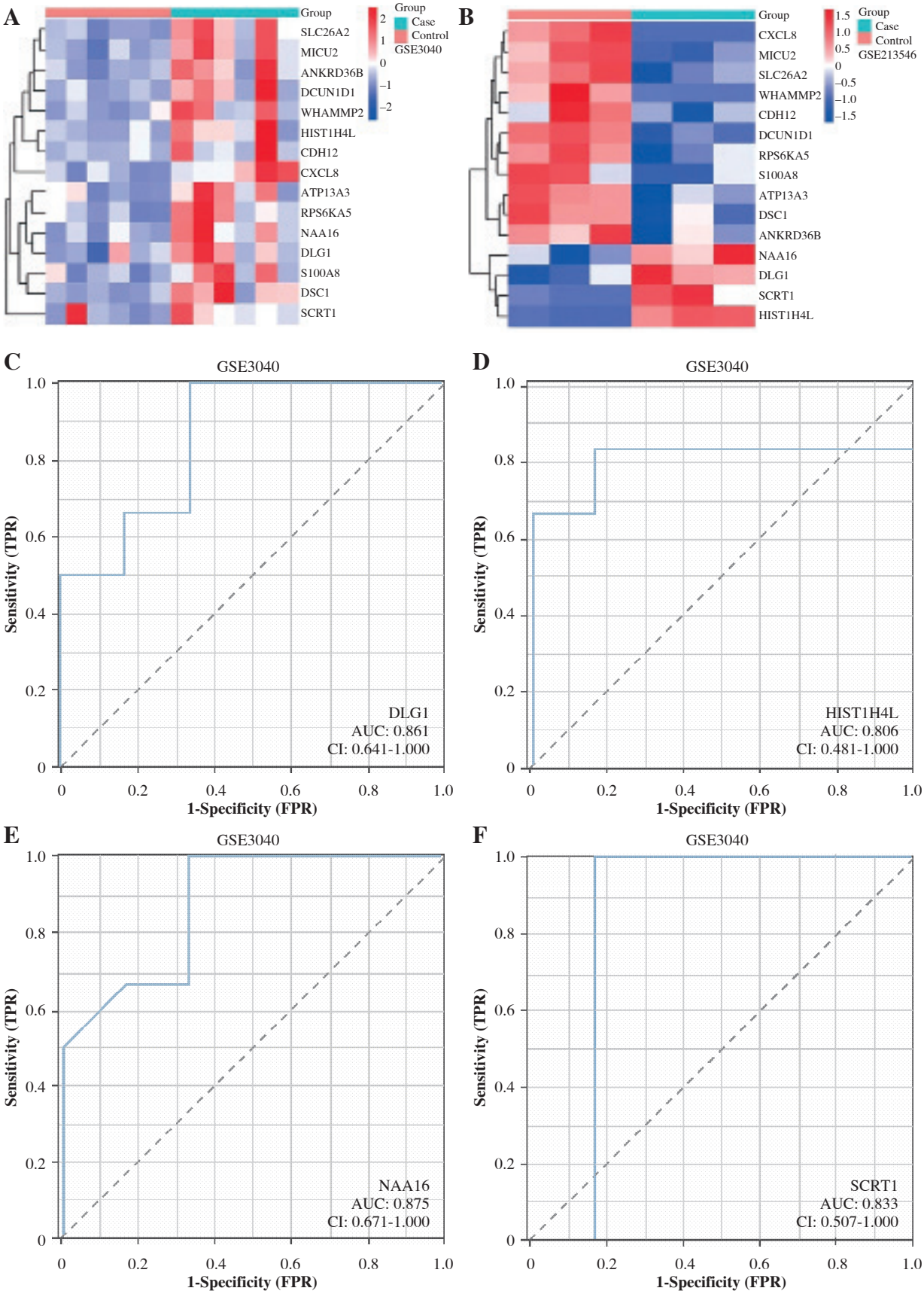

Fig. 2. Expression and receiver operating characteristic (ROC) analysis of overlapping genes in the GSE3040 and GSE213546 datasets. **A**, **B**) Heatmaps showing the expression levels of 15 overlapping genes in case and control samples from the GSE3040 (**A**) and GSE213546 (**B**) datasets. Red indicates high expression, and blue indicates low expression. **C-F**) ROC curves for *DLG1* (**C**), *HIST1H4L* (**D**), *NAA16* (**E**), and *SCRT1* (**F**) in the GSE3040 dataset.

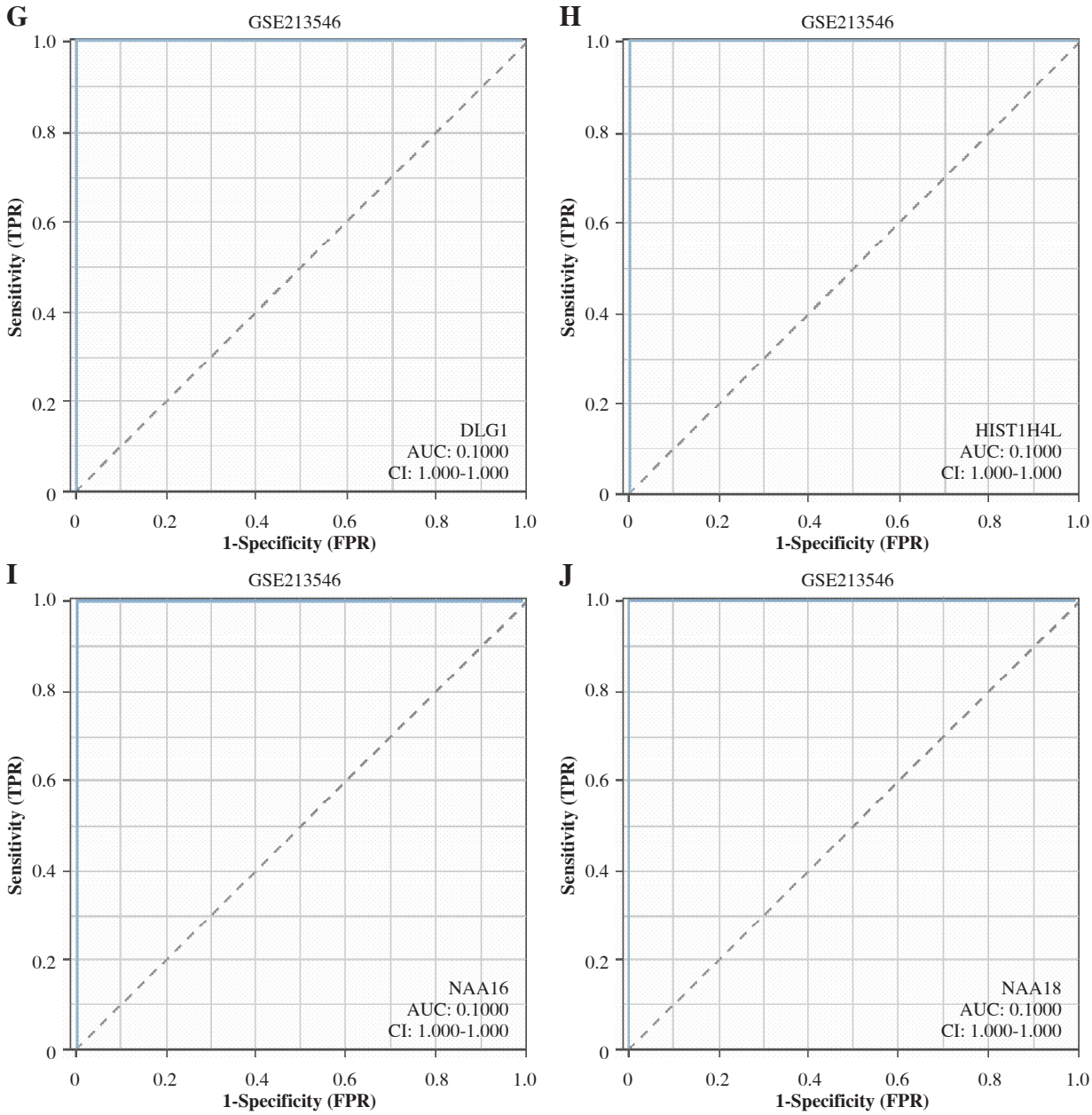

Fig. 2. Cont. **G-J**) ROC curves for *DLG1* (**G**), *HIST1H4L* (**H**), *NAA16* (**I**), and *SCRT1* (**J**) in the GSE213546 dataset. The area under the curve (AUC) and 95% CI are indicated in the lower right corner of each figure. *DLG1* – discs large MAGUK scaffold protein 1, *HIST1H4L* – histone H4, *NAA16* – N-alpha-acetyltransferase 16, NatA auxiliary subunit, *SCRT1* – Scratch family transcriptional repressor 1

DLG1, HIST1H4L, NAA16, and SCRT1 are upregulated in ARC

Subsequently, the expression of 15 overlapping genes in different groups of the GSE3040 and GSE213546 datasets was analyzed (Fig. 2A, B). Among them, *DLG1*, histone H4 (*HIST1H4L*), N alpha acetyltransferase 16 (*NAA16*), and Scratch family transcriptional repressor 1 (*SCRT1*) showed consistent upregulation in the case groups of both datasets. In ROC analysis of GSE3040, the AUC values for *DLG1*, *HIST1H4L*, *NAA16*, and *SCRT1* were 0.861, 0.806, 0.875, and 0.833, respectively (Fig. 2C-F). In GSE213546, the AUCs for all four genes reached 1.000 (Fig. 2G-J), indicating excellent discrimination between cataract and control samples. Further validation using qRT-PCR in HLECs showed that H_2O_2 treatment signifi-

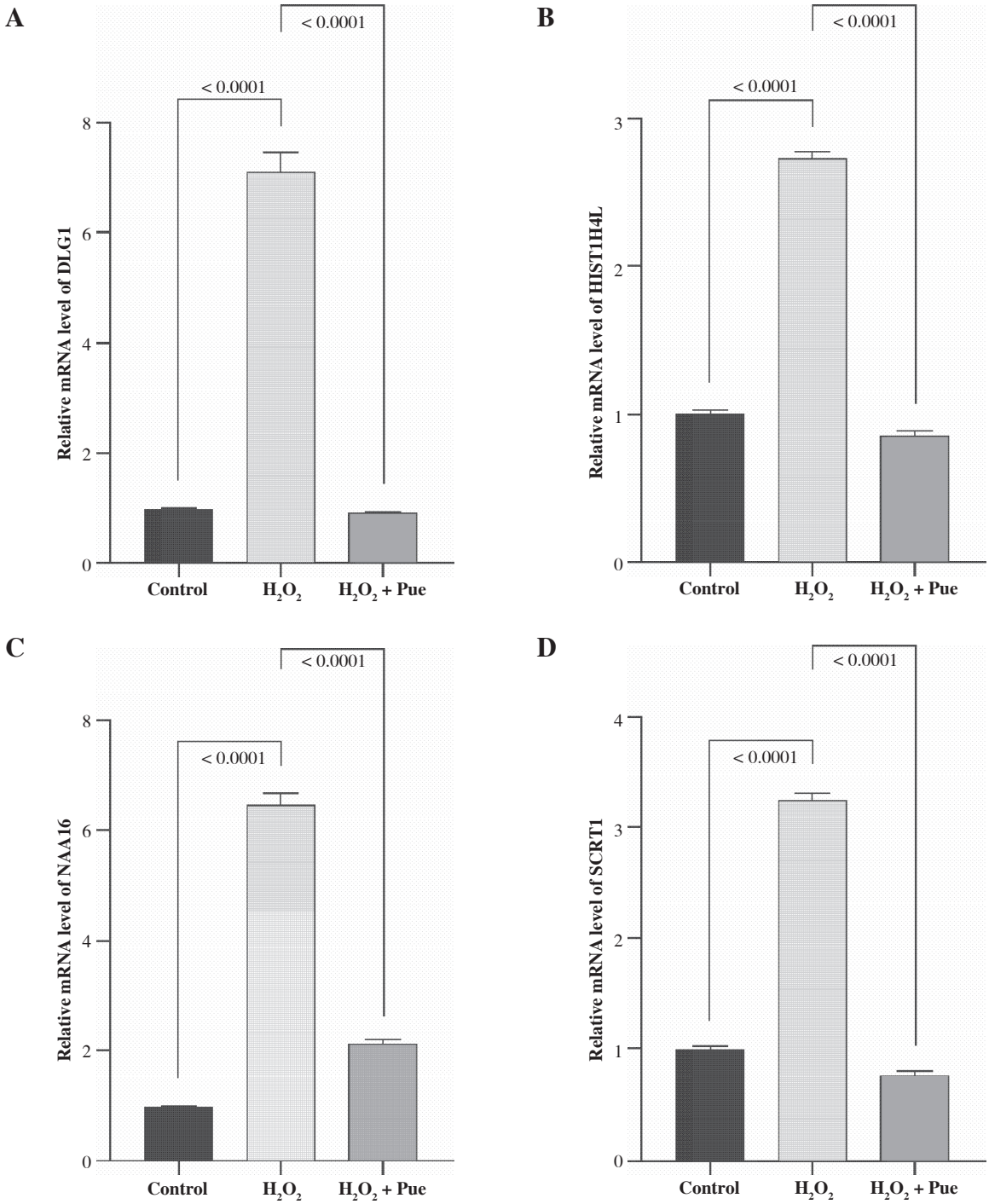

Fig. 3. Quantitative real-time polymerase chain reaction (qRT-PCR) analysis of the effects of puerarin (Pue) on the expression of *DLG1*, *HIST1H4L*, *NAA16*, and *SCRT1* in H_2O_2-induced HLECs. **A**) Relative *DLG1* mRNA expression in human corneal endothelial cells (HLECs) across control, H_2O_2, and H_2O_2 + Pue (50 μM) groups. **B**) Relative *HIST1H4L* mRNA expression in HLECs under the same conditions. **C**) Relative *NAA16* mRNA expression in HLECs under the same conditions. **D**) Relative *SCRT1* mRNA expression in HLECs under the same conditions. Data were collected from three biologically independent replicates. HLECs – human lens epithelial cells, *DLG1* – discs large MAGUK scaffold protein 1, *HIST1H4L* – histone H4, *NAA16* – N-alpha-acetyltransferase 16, NatA auxiliary subunit, *SCRT1* – Scratch family transcriptional repressor 1

cantly upregulated the mRNA levels of *DLG1*, *HIST1H4L*, *NAA16*, and *SCRT1*, and this effect was reversed by co-treatment with Pue (Fig. 3A-D). These results suggest that *DLG1*, *HIST1H4L*, *NAA16*, and *SCRT1* not only have robust diagnostic potential in ARC, but also participate in oxidative stress-related molecular alterations and can be modulated by Pue.

DLG1 regulates oxidative stress-induced cell damage in HLECs

After HLECs were induced with H_2O_2 to establish the model, H_2O_2 exposure significantly increased the mRNA and protein levels of *DLG1* compared with the control group (Fig. 4A-C). Among the three siRNAs, si-*DLG1*-1 showed the highest knockdown efficiency, as reflected

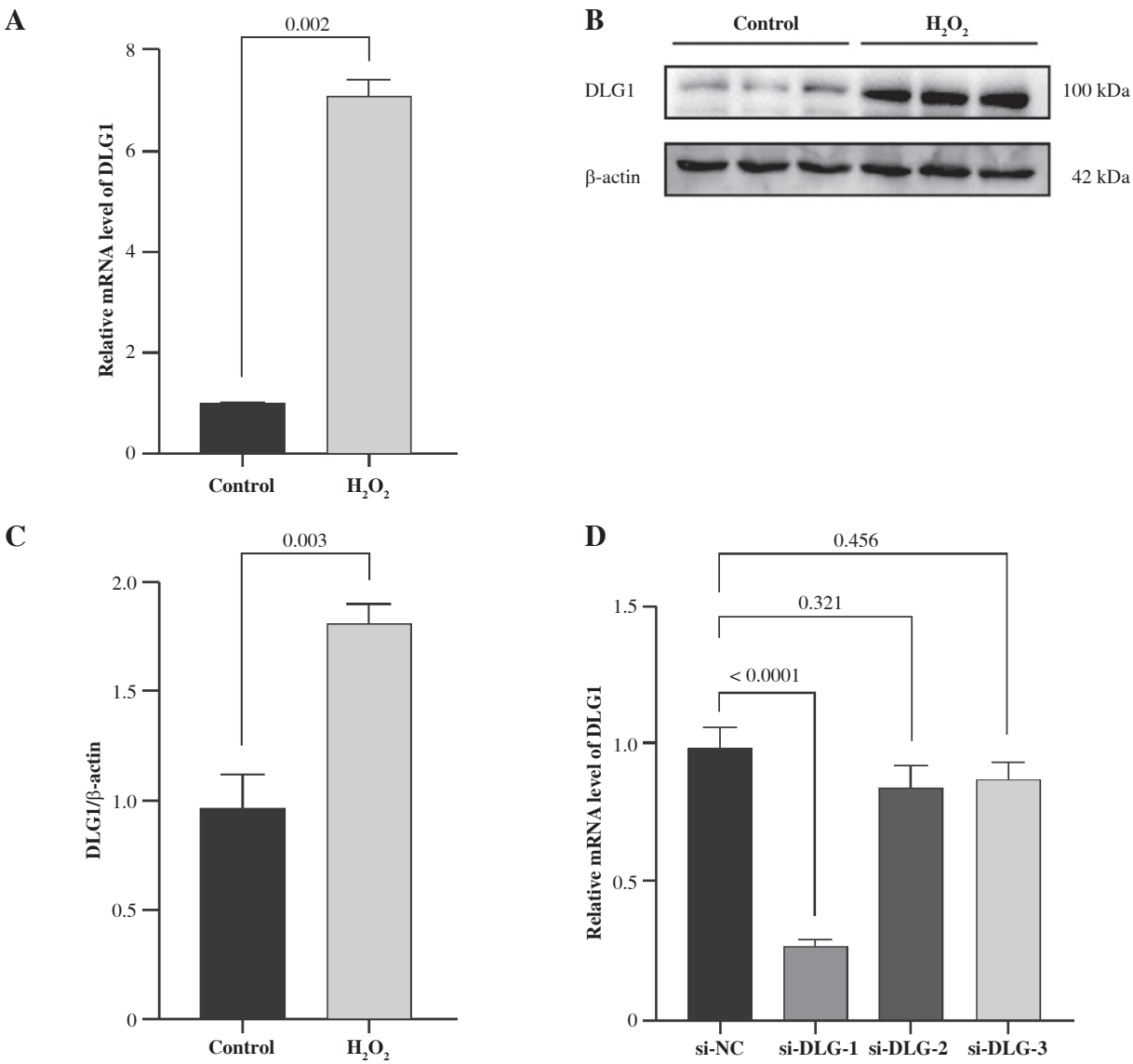

Fig. 4. Effects of knockdown or overexpression of *DLG1* on the viability of human lens epithelial cells (HLECs) treated with H_2O_2. **A**) Quantitative real-time polymerase chain reaction (qRT-PCR) analysis shows the mRNA level of *DLG1* in HLECs after H_2O_2 treatment. **B**) Western blot analysis of DLG1 protein expression in HLECs, with and without H_2O_2 treatment; β-actin was used as a loading control. **C**) Quantification of band intensity in panel B, and calculation of the relative expression level of DLG1/β-actin after normalization with β-actin. **D**) qRT-PCR analysis was used to evaluate the knockdown efficiency of *DLG1* mRNA in HLECs after transfection with si-*DLG1*-1/-2/-3 and si-NC using Lipofectamine RNAiMAX. Data were collected from three biologically independent replicates. *DLG1* – discs large MAGUK scaffold protein 1, siRNAs – small interfering RNAs

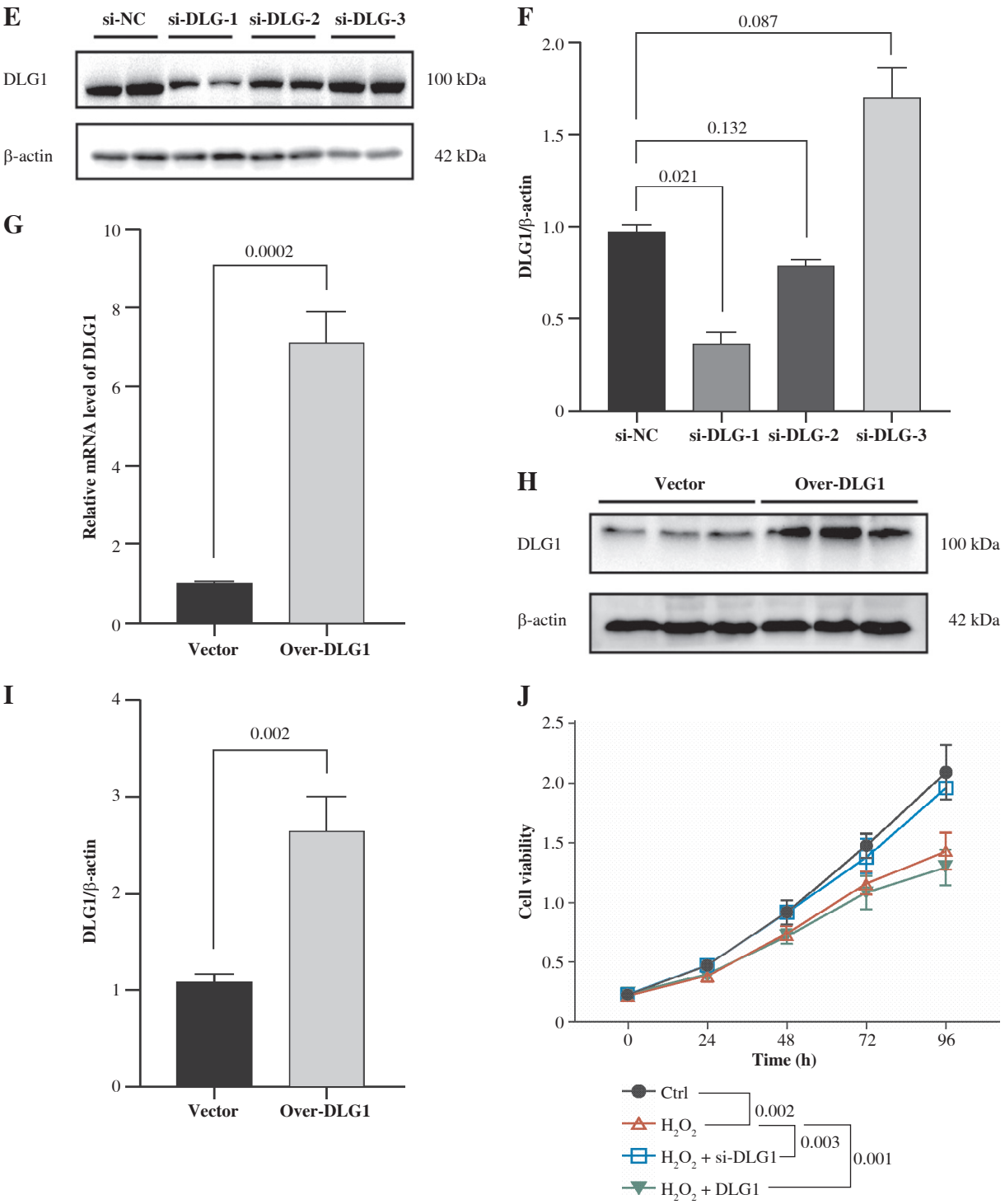

Fig. 4. Cont. **E**) Western blot analysis of DLG1 protein knockdown efficiency in HLECs using si-*DLG1*-1/-2/-3; β-actin was used as a loading control. **F**) Quantification of band intensity in panel E, followed by normalization with β-actin to determine the relative expression level of DLG1/β-actin. **G**) qRT-PCR validation of the upregulation of *DLG1* mRNA in HLECs after transfection with over-*DLG1* and empty vector using Lipofectamine 3000. **H**) Western blot validation of the upregulation of DLG1 protein by the over-*DLG1* vector compared to the empty vector; β-actin was used as a loading control. **I**) Quantification of band intensity in panel H, followed by normalization with β-actin to determine the relative expression level of DLG1/β-actin. **J**) Cell viability assay shows the changes in HLECs' viability after *DLG1* knockdown or overexpression under H_2O_2-induced oxidative stress. Data were collected from three biologically independent replicates. *DLG1* – discs large MAGUK scaffold protein 1, siRNAs – small interfering RNAs

by the reduction of *DLG1* mRNA and protein levels, and was therefore used in subsequent experiments (Fig. 4D-F). qRT-PCR and Western blot analysis also verified the effectiveness of transfected overexpressed *DLG1* (Fig. 4G-I). Further functional experiments (Fig. 4J) demonstrated that under H_2O_2-induced oxidative stress, *DLG1* silencing resulted in a substantial reduction in cell viability, indicating that *DLG1* may play a pro-survival role during oxidative stress. Conversely, *DLG1* overexpression significantly increased cell viability and, to some extent, offset the cell damage induced by H_2O_2 treatment. These findings indicate that *DLG1* may be involved in ARC-related HLEC damage by modulating cell survival under oxidative stress.

Pue attenuates oxidative stress-induced HLEC damage and DLG1 upregulation

Molecular docking analysis demonstrated that Pue has a high affinity for *DLG1* (Fig. 5A). Pue treatment alone

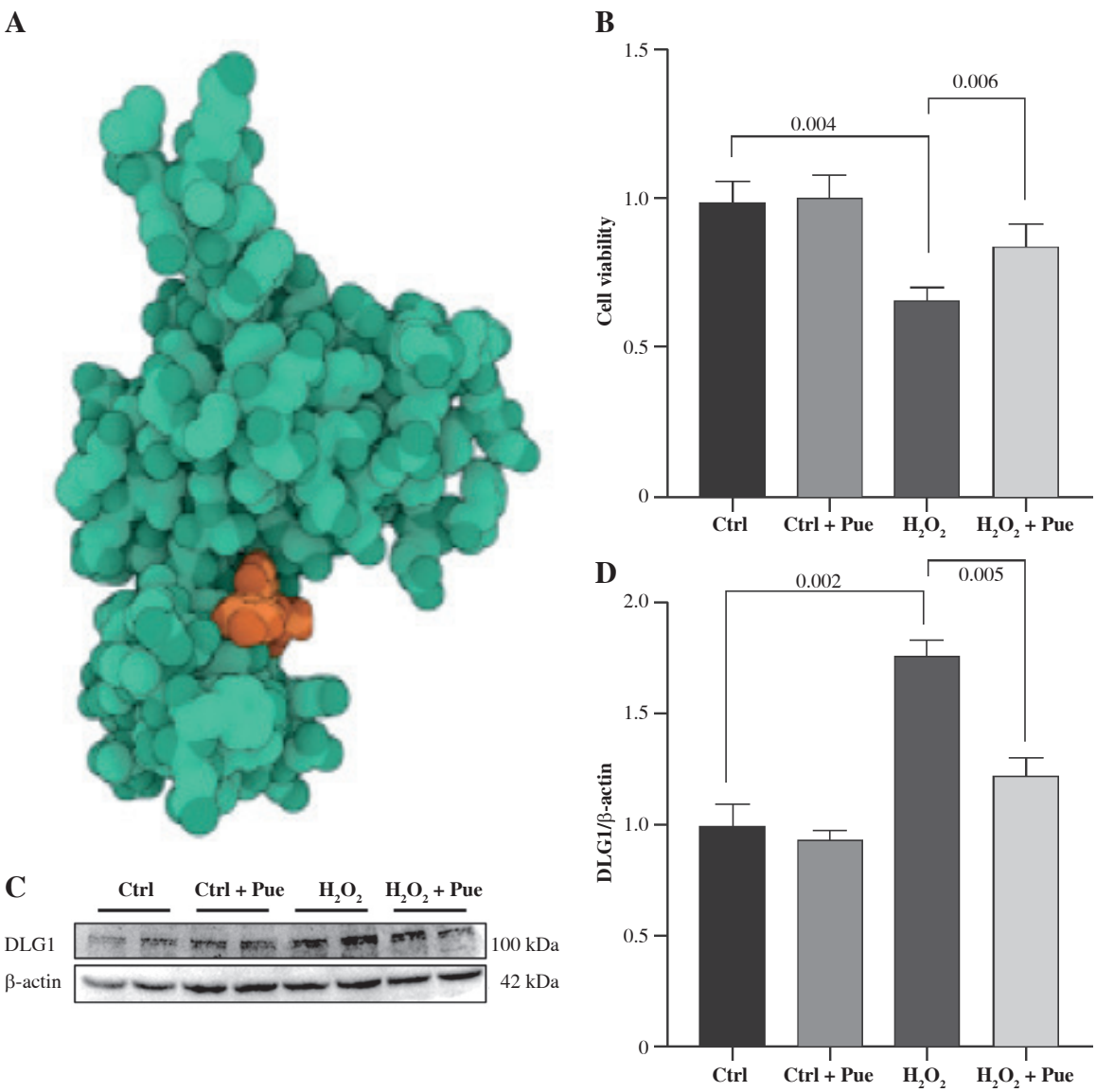

Fig. 5. Puerarin (Pue) alleviates H_2O_2-induced decreases in HLEC cell viability and DLG1 protein expression. **A**) Molecular docking model showing the binding of Pue (orange) to *DLG1* (green). **B**) Cell Counting Kit-8 (CCK-8) assay assessing cell viability of HLECs in different treatment groups (Control [Ctrl], Ctrl + Pue (50 μM), H_2O_2, and H_2O_2 + Pue (50 μM)). **C**) Representative Western blot images of DLG1 and β-actin in different treatment groups. **D**) Quantification of DLG1 protein levels normalized to β-actin. Data were collected from three biologically independent replicates. HLECs – human lens epithelial cells, *DLG1* – discs large MAGUK scaffold protein 1

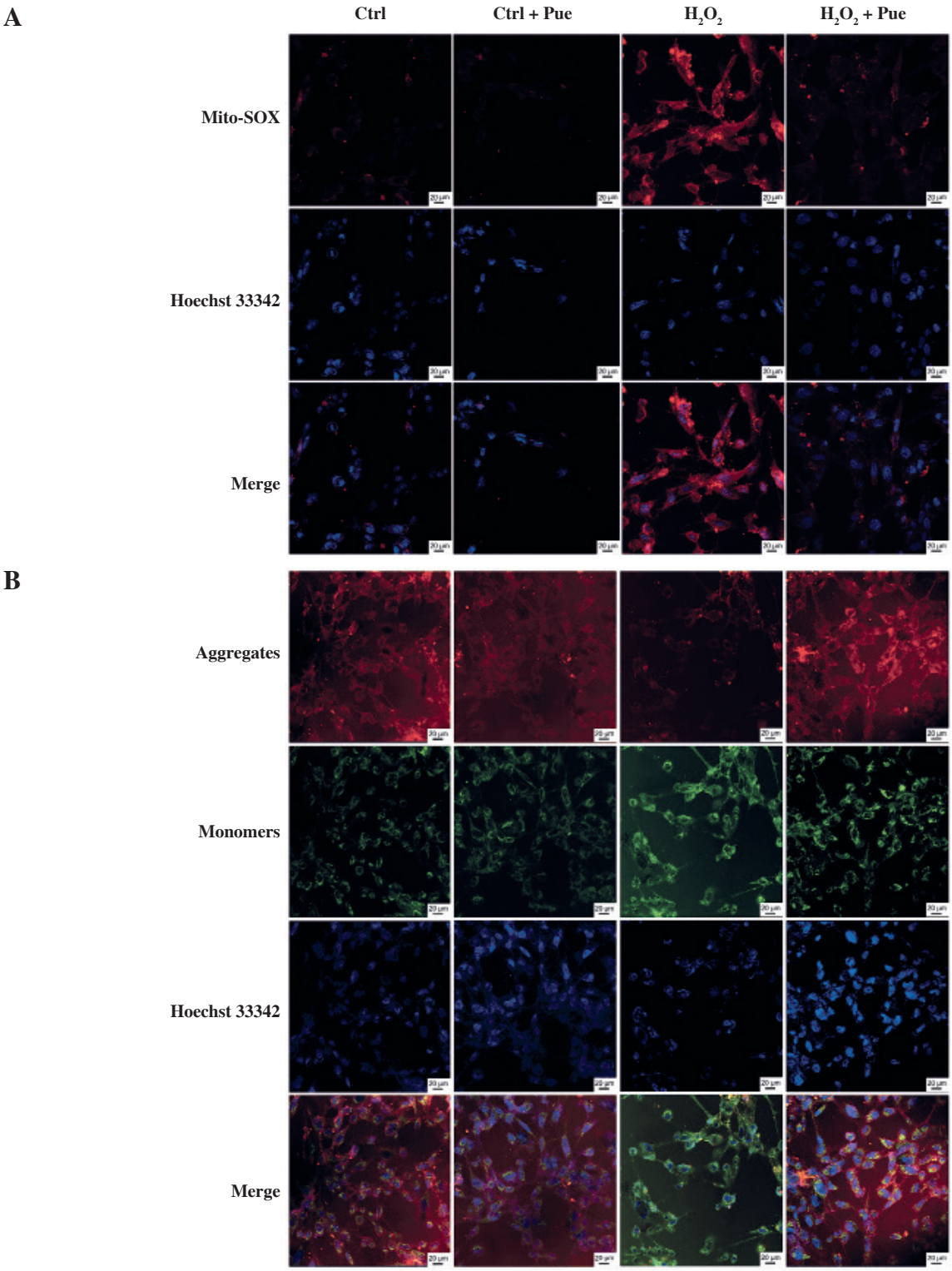

Fig. 6. Effects of puerarin (Pue) on mitochondrial reactive oxygen species (ROS) and mitochondrial membrane potential (MMP) in human lens epithelial cells (HLECs). **A**) Representative MitoSOX staining images of the Control (Ctrl), Ctrl + Pue (50 μM), H_2O_2, and H_2O_2 + Pue (50 μM) groups. Mitochondrial ROS are visualized in red, and nuclei are counterstained with Hoechst 33342 (blue). "Merge" represents the overlay of the two channels. **B**) JC-1 staining shows mitochondrial aggregates (red) and monomers (green) for assessment of MMP. Hoechst 33342 nuclear staining is shown (blue). Data were collected from three biologically independent replicates

did not significantly alter cell viability as compared to the control group. However, when combined with H_2O_2 exposure, Pue markedly reversed the H_2O_2-induced reduction in HLEC viability (Fig. 5B). Western blot analysis showed that H_2O_2 treatment significantly increased DLG1 protein expression, while Pue treatment significantly inhibited H_2O_2-induced DLG1 upregulation (Fig. 5C, D). These results suggest that Pue may protect HLECs from oxidative stress-induced cell damage by modulating *DLG1* expression.

Pue alleviates mitochondrial dysfunction in HLECs induced by oxidative stress

In comparison with the control group, H_2O_2 treatment considerably increased mitochondrial ROS generation, while Pue therapy dramatically decreased H_2O_2-induced ROS accumulation, according to mito-SOX staining (Fig. 6A). JC-1 staining showed that H_2O_2 markedly reduced MMP, reflected by lower red (aggregates) and higher green (monomers) fluorescence. In comparison to the H_2O_2 group, the red/green fluorescence ratio was increased, indicating that the Pue treatment successfully preserved MMP (Fig. 6B). These findings indicate that Pue can mitigate mitochondrial oxidative damage and preserve mitochondrial function in HLECs subjected to oxidative stress.

DLG1 overexpression attenuates the protective effect of Pue against oxidative stress-induced mitochondrial dysfunction in HLECs

According to earlier research, Pue has a significant regulatory effect in suppressing inflammation as well as restoring mitochondrial function [29, 30]. To further determine whether *DLG1* mediates the protective effect of Pue against oxidative stress in HLECs, we overexpressed *DLG1* using plasmid transfection. Cell viability exper-

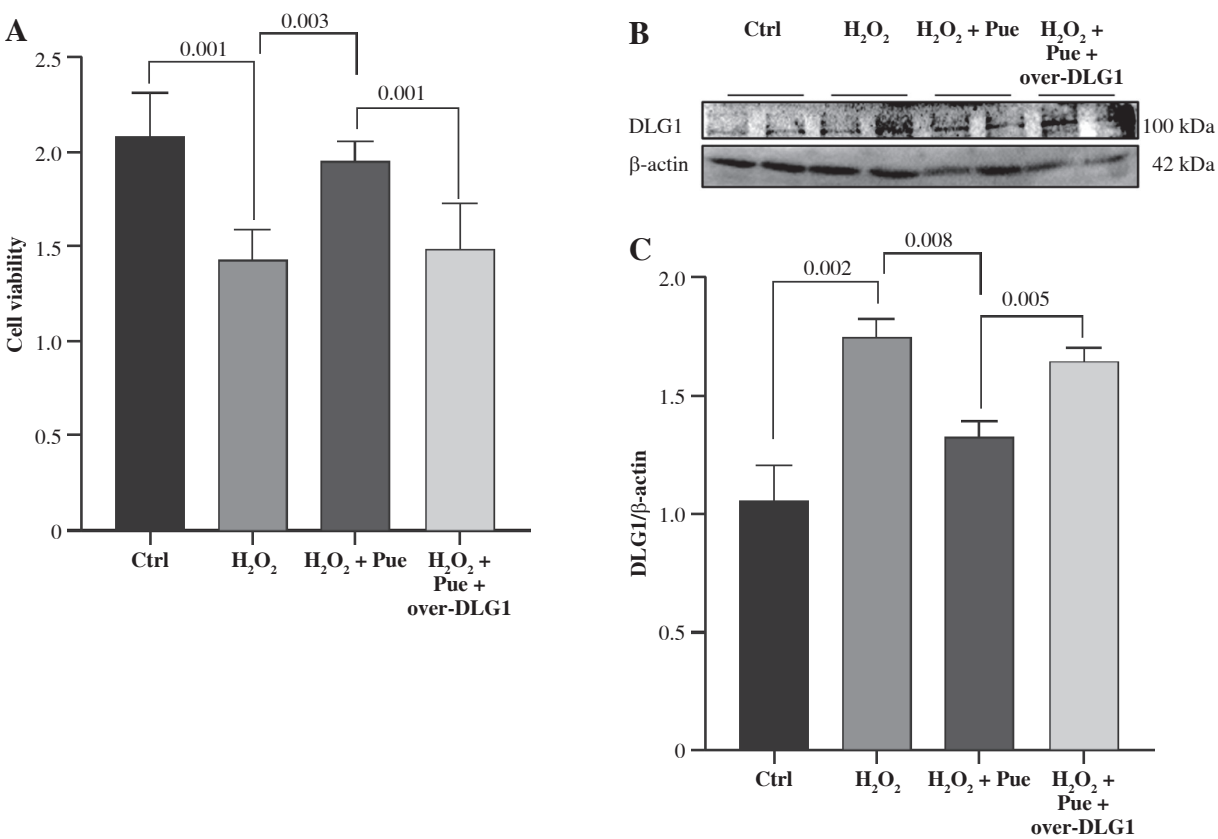

Fig. 7. *DLG1* overexpression attenuates the protective effect of puerarin (Pue) against oxidative stress-induced mitochondrial dysfunction in human lens epithelial cells (HLECs). **A**) Cell viability was assessed using the Cell Counting Kit-8 (CCK-8) assay in Control (Ctrl), H_2O_2, H_2O_2 + Pue (50 μM), and H_2O_2 + Pue (50 μM) + *DLG1* groups. **B**, **C**) Western blot analysis and quantification of DLG1 protein levels. β-actin was used as a loading control. Red fluorescence indicates JC-1 aggregates (high MMP), and green fluorescence indicates JC-1 monomers (low MMP). Data were collected from three biologically independent replicates. *DLG1* – discs large MAGUK scaffold protein 1

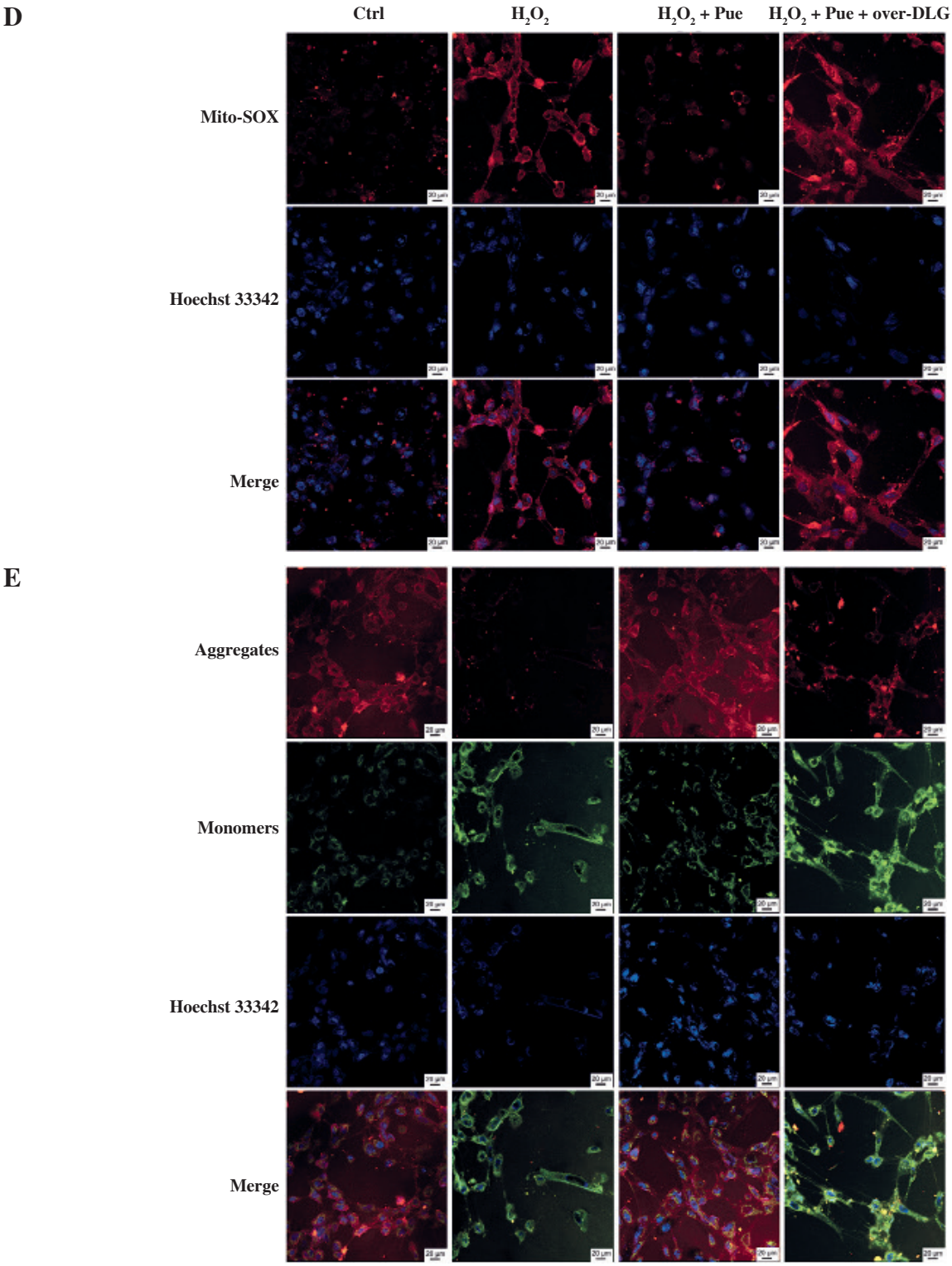

Fig. 7. Cont. **D**) Representative immunofluorescence images of mitochondrial reactive oxygen species (ROS) production detected using MitoSOX staining (red). Nuclei were counterstained with Hoechst 33342 (blue). **E**) JC-1 staining showing mitochondrial membrane potential (MMP) changes. Red fluorescence indicates JC-1 aggregates (high MMP), and green fluorescence indicates JC-1 monomers (low MMP). Data were collected from three biologically independent replicates. *DLG1* – discs large MAGUK scaffold protein 1

iments revealed that Pue protected HLECs from H_2O_2-induced viability loss, while overexpression of *DLG1* significantly attenuated this protective effect (Fig. 7A). Western blot analysis showed that Pue treatment reversed the upregulation of DLG1 expression in the H_2O_2 group. However, overexpression of DLG1 reversed the inhibitory effect of Pue, restoring DLG1 protein levels to levels close to those in the H_2O_2 group (Fig. 7B, C). Mito-SOX staining revealed that Pue treatment significantly attenuated H_2O_2-induced mitochondrial ROS accumulation, while overexpression of *DLG1* reversed this effect (Fig. 7D). Furthermore, JC-1 staining revealed that Pue restored the H_2O_2-induced decrease in mitochondrial membrane potential, while overexpression of *DLG1* counteracted this effect, as demonstrated by an increase in the ratio of red fluorescence (aggregates) to green fluorescence (monomers) (Fig. 7E). These results suggest that Pue alleviates oxidative stress-induced mitochondrial dysfunction in HLECs, at least in part, by inhibiting the upregulation of *DLG1*.

Discussion

Age-related cataract, also known as senile cataracts, is primarily caused by aging and lens deterioration [31]. With aging, excessive ROS production in lens epithelial cells leads to oxidative damage to proteins, lipids, and nucleic acids, ultimately causing lens opacity, primarily manifesting as decreased vision and blurred vision [32]. Research on key regulatory genes of cataracts and their potential biomarkers is increasing. These biomarkers are crucial for uncovering the molecular mechanisms of cataracts and promoting early diagnosis. For example, a meta-analysis investigated the association between crystallin alpha A (*CRYAA*) gene polymorphisms and cataract susceptibility and found that carriers of the rs7278468 polymorphism had a significantly reduced risk of cataract [33]. A study by Wu *et al*. [34] demonstrated that glutathione S-transferase pi 1 (*GSTP1*) expression is markedly decreased in the lenses of ARC patients and Emory mice. This gene promotes mitochondrial fusion by upregulating the mitochondrial fusion-related proteins mitofusin 1/2 (*MFN1/2*), thus providing a potential therapeutic target for ARC. In another ARC study, the antioxidant genes *GSTP1* and thioredoxin reductase 2 (*TXNRD2*) were also shown to help mitigate oxidative damage in the lens [35]. Therefore, intervention targeting molecular targets related to oxidative stress may offer novel strategies for ARC treatment.

This study integrated bioinformatics analysis data from two independent GEO databases and identified 15 overlapping genes. Enrichment analysis revealed that these genes were enriched in pathways related to neutrophil chemotaxis, cellular responses to interleukin-1, calcium ion binding, RAGE receptor binding, histone H3 kinase activity, and adherens junctions. Further expression analysis revealed that four genes (*DLG1*, *HIST1H4L*, *NAA16*, and *SCRT1*) were upregulated in ARC samples in both the GSE3040 and GSE213546 datasets, and exhibited high diagnostic performance in ROC analysis. In pan-cancer genetic analyses, *HIST1H4L* was identified as a pleiotropic susceptibility gene for esophageal and lung cancers, and showed potential regulatory roles in multi-tissue analyses integrating eQTL data [36]. Aberrant methylation/expression of *HIST1H4L* was significantly associated with Parkinson's disease [37]. Through genome-wide and Mendelian randomization analyses, *NAA16* was identified as a gene potentially causally associated with traumatic brain injury (TBI), suggesting that *NAA16* may participate in the "gut microbiota-host" regulatory axis influencing TBI susceptibility/progression [38]. *SCRT1* is highly expressed in the cluster B subtype of glioblastoma, which also exhibits low expression of immune-related genes and low immunogenicity, suggesting that *SCRT1* may mark an immunosuppressive tumor microenvironment [39]. Furthermore, research has shown that *SCRT1* expression in pancreatic β-cells positively correlates with insulin secretion capacity and INS gene expression, and is downregulated in β-cells of type 2 diabetes (T2D) patients. Knockdown of *SCRT1* impairs glucose-stimulated insulin secretion and reduces Ins1/multiple key β-cell transcription factor expression; its activity is regulated by glucose and GSK3β-dependent phosphorylation, suggesting it as a potential biomarker/therapeutic target for β-cell dysfunction and T2D [40]. At present, these genes have not been systematically investigated in ophthalmic diseases; therefore, further studies are needed to elucidate their ARC-specific roles and potential clinical value.

By scavenging free radicals and lowering oxidative stress, Pue flavonoids have anti-inflammatory and antioxidant properties [24]. Importantly, accumulating evidence indicates that the protective effects of Pue are closely associated with its ability to suppress ROS generation and preserve mitochondrial function. A study showed that Pue protects mitochondrial function by inhibiting oxidative stress, preventing cadmium (Cd)-induced mitochondrial ultrastructural damage, as well as alleviating cytotoxicity in AML-12 mouse hepatocytes by restoring mitochondrial network fragmentation [41]. In addition, Pue has been reported to alleviate cerebral ischemia/reperfusion (CIR)-induced neuronal oxidative stress and apoptosis [42]. Furthermore, Pue inhibits spinal Src activity, thereby restoring mitochondrial function and attenuating cancer-induced bone pain [43]. Given that excessive ROS production and mitochondrial dysfunction are central events in ARC pathogenesis, these findings suggest that Pue may exert similar protective effects in lens epithelial cells. Our study demonstrated that in H_2O_2-induced HLECs, the expression levels of *DLG1*, *HIST1H4L*, *NAA16*, and *SCRT1* were upregulated, and this upregu-

lation could be partially reversed by treatment with Pue. Notably, Pue significantly reduced mitochondrial ROS levels and restored mitochondrial membrane potential, indicating that its protective effect is largely mediated through attenuation of oxidative stress and preservation of mitochondrial integrity.

Given that *DLG1*, *HIST1H4L*, *NAA16*, and *SCRT1* were induced by H_2O_2 and partly reversed by Pue treatment in HLECs, we next focused on *DLG1* as a putative mediator of Pue's effects. A previous study suggested that claudin 6 (*CLDN6*) may contribute to ferroptosis-associated oxidative stress and mitochondrial dysfunction through the DLG1/PBK complex in breast cancer [44]. In addition, p38γ has been reported to regulate lipid accumulation and oxidative stress *via DLG1* in liver injury [45]. Together, these studies further support the involvement of DLG1 in oxidative stress-related pathological processes. *In vitro* experiments revealed that *DLG1* expression was significantly upregulated after H_2O_2 induction, and its silencing reduced cell viability damage under oxidative stress, while overexpression had the opposite effect, suggesting that DLG1 may amplify oxidative stress-induced cellular injury in ARC. Molecular docking analysis demonstrated that Pue has a high binding affinity for *DLG1*. Pue treatment significantly suppressed DLG1 upregulation induced by oxidative stress, accompanied by reduced ROS accumulation and improved mitochondrial function. Further experiments showed that DLG1 overexpression attenuated the protective effects of Pue against oxidative stress and mitochondrial dysfunction, suggesting that DLG1 may function as a key downstream mediator of Pue-induced antioxidant and mitochondria-protective effects.

By integrating bioinformatics analysis and cell experiments, this study identified *DLG1* as a potential mediator of oxidative stress-induced damage in ARC and characterized the protective effects of Pue. Our findings suggest that DLG1 upregulation contributes to ROS accumulation and mitochondrial dysfunction in HLECs, thereby aggravating ARC-related cellular injury. Pue attenuates these effects by suppressing DLG1 expression, reducing oxidative stress, and preserving mitochondrial function. However, the study has some limitations. First, this study only established an *in vitro* H_2O_2-induced HLEC model and has not been validated in an animal model. Second, although the expression levels of four candidate genes (*DLG1*, *HIST1H4L*, *NAA16*, and *SCRT1*) were consistently elevated and had diagnostic value, we only performed functional experiments on *DLG1*; the mechanisms of the other genes require further investigation. Third, while molecular docking and functional experiments suggest that baicalin may regulate *DLG1*, its precise molecular mechanism remains to be elucidated. Furthermore, this study did not systematically evaluate the pharmacokinetics of baicalin at different doses and administration times; therefore, further research is needed.

Conclusions

In summary, this study identified *DLG1* as a potential contributor to oxidative stress-induced damage in ARC. Pue alleviated oxidative stress-induced HLEC damage and mitochondrial dysfunction, at least in part, by attenuating *DLG1* upregulation. Mechanistically, Pue may exert its protective effects by reducing mitochondrial ROS production and maintaining mitochondrial membrane potential. These findings suggest that *DLG1* may represent a potential therapeutic target in ARC and that Pue is a promising candidate for further investigation as an intervention for ARC.

Funding

The Natural Science Research Project of the Anhui Provincial Department of Education, China (2025AHGXZK20106, Major Project). The Scientific Research Startup Fund Project for High-level Talents of the Second Affiliated Hospital of Wannan Medical College (GRK202507). The Natural Science Foundation project of Wannan Medical College (No. EYR202201).

Disclosures

Approval of the Bioethics Committee was not required. The authors declare no conflict of interest.

Supplementary material is available on the journal's website.

References

1. Cicinelli MV, Buchan JC, Nicholson M, et al. (2023): Cataracts. Lancet 401: 377-389.
2. Falkowska M, Młynarczyk M, Micun Z, et al. (2023): Influence of diet, dietary products and vitamins on age-related cataract incidence: a systematic review. Nutrients 15: 4585.
3. Hejtmancik JF (2024): Oxidative stress in genetic cataract formation. Antioxidants 13: 1315.
4. Zhang L, Zhang ZF, Hui YN, et al. (2024): Oxidative stress participates in age-related cataract formation by disrupting connection between lens epithelial cells through c-src/VEGF pathway. Curr Eye Res 49: 380-390.
5. Nsonwu M, Ozims S, Nnodim J (2024): Perspective of cataract and oxidative stress. Series Clin Biomed Res 1: 1-10.
6. Lim JC, Jiang L, Lust NG, Donaldson PJ (2024): Minimizing oxidative stress in the Lens: alternative measures for elevating glutathione in the Lens to protect against cataract. Antioxidants 13: 1193.
7. Lim JC, Grey AC, Zahraei A, Donaldson PJ (2020): Age-dependent changes in glutathione metabolism pathways in the lens: new insights into therapeutic strategies to prevent cataract formation – a review. Clin Exp Ophthalmol 48: 1031-1042.
8. Qin Y, Liu H, Wu H (2025): Cellular senescence in health, disease, and lens aging. Pharmaceuticals 18: 244.

9. Babizhayev MA, Yegorov YE (2016): Reactive oxygen species and the aging eye: Specific role of metabolically active mitochondria in maintaining lens function and in the initiation of the oxidation-induced maturity onset cataract – A novel platform of mitochondria-targeted antioxidants with broad therapeutic potential for redox regulation and detoxification of oxidants in eye diseases. Am J Ther 23: e98-e117.
10. Marziali F, Dizanzo MP, Cavatorta AL, Gardiol D (2019): Differential expression of DLG1 as a common trait in different human diseases: an encouraging issue in molecular pathology. Biol Chem 400: 699-710.
11. Rivera C, Yamben IF, Shatadal S, et al. (2009): Cell-autonomous requirements for Dlg-1 for lens epithelial cell structure and fiber cell morphogenesis. Dev Dyn 238: 2292-2308.
12. Peng Z, Li X, Li J, et al. (2021): Dlg1 knockout inhibits microglial activation and alleviates lipopolysaccharide-induced depression-like behavior in mice. Neurosci Bull 37: 1671-1682.
13. Li X, Peng Z, Jiang L, et al. (2023): Dlg1 deletion in microglia ameliorates chronic restraint stress induced mice depression-like behavior. Front Pharmacol 14: 1124845.
14. Chang H, Wu H, Hou P, et al. (2023): DLG1 promotes the antiviral innate immune response by inhibiting p62-mediated autophagic degradation of IKKε. J Virol 97: e01501-e01523.
15. He H, Peng S, Song X, et al. (2022): Protective effect of isoflavones and triterpenoid saponins from pueraria lobata on liver diseases: A review. Food Sci Nutr 10: 272-285.
16. Xia J, Zhou M, Ma Y, et al. (2025): Puerarin alleviates high glucose-induced lens epithelial cell damage by activating the Nrf2 Signaling pathway to inhibit oxidative stress. Toxicol Res (Camb) 14: tfaf109.
17. Wan Q, Lu Q, Luo S, et al. (2024): The beneficial health effects of puerarin in the treatment of cardiovascular diseases: from mechanisms to therapeutics. Naunyn Schmiedebergs Arch Pharmacol 397: 7273-7296.
18. Wang D, Bu T, Li Y, et al. (2022): Pharmacological activity, pharmacokinetics, and clinical research progress of puerarin. Antioxidants 11: 2121.
19. Zhou YX, Zhang H, Peng C (2021): Effects of puerarin on the prevention and treatment of cardiovascular diseases. Front Pharmacol 12: 771793.
20. Zhou Y, Zhang H, Peng C (2024): Cardiovascular actions and therapeutic potential of puerarin. Authorea Preprints.
21. Yu CC, Du YJ, Li J, et al. (2022): Neuroprotective mechanisms of puerarin in central nervous system diseases: update. Aging Dis 13: 1092-1105.
22. He YX, Liu MN, Wu H, et al. (2024): Puerarin: a hepatoprotective drug from bench to bedside. Chin Med 19: 139.
23. Meng F, Guo B, Ma YQ, et al. (2022): Puerarin: A review of its mechanisms of action and clinical studies in ophthalmology. Phytomedicine 107: 154465.
24. Jeon YD, Lee JH, Lee YM, Kim DK (2020): Puerarin inhibits inflammation and oxidative stress in dextran sulfate sodium-induced colitis mice model. Biomed Pharmacother 124: 109847.
25. Xu J, Li X, Sun F (2010): Preparation and evaluation of a contact lens vehicle for puerarin delivery. J Biomater Sci Polym Ed. 21: 271-288.
26. Gupta V, Galante A, Soteropoulos P, et al. (2005): Global gene profiling reveals novel glucocorticoid induced changes in gene expression of human lens epithelial cells. Mol Vis 11: 1018-1040.
27. Fu L, Yang Q, Han Y, et al. (2025): Slit2 promotes H(2)O(2)-induced lens epithelial cells oxidative damage and age-related cataract. Curr Eye Res 50: 41-50.
28. Chen Z, Halford NG, Liu C (2023): Real-time quantitative PCR: Primer design, reference gene selection, calculations and statistics. Metabolites 13: 806.
29. Zhang L, Liu L, Wang M (2021): Effects of puerarin on chronic inflammation: Focus on the heart, brain, and arteries. Aging Med (Milton) 4: 317-324.
30. Wang YS, Li BY, Xing YF, et al. (2024): Puerarin ameliorated PCOS through preventing mitochondrial dysfunction dependent on the maintenance of intracellular calcium homeostasis. J Agric Food Chem 72: 2963-2976.
31. Mishra D, Kashyap A, Srivastav T, et al. (2023): Enzymatic and biochemical properties of lens in age-related cataract versus diabetic cataract: A narrative review. Indian J Ophthalmol 71: 2379-2384.
32. Huang Y, Liu Y, Yu S, et al. (2022): Biliverdin reductase a protects lens epithelial cells against oxidative damage and cellular senescence in age-related cataract. Oxid Med Cell Longev 2022: 5628946.
33. Yu H, Liu K, Lu P (2021): Polymorphisms in CRYAA promoter with susceptibility to cataract: a meta-analysis. Semin Ophthalmol 36: 429-436.
34. Wu A, Zhang W, Zhang G, et al. (2023): Age-related cataract: GSTP1 ubiquitination and degradation by Parkin inhibits its anti-apoptosis in lens epithelial cells. Biochim Biophys Acta Mol Cell Res 1870: 119450.
35. Zhu X, Li D, Du Y, et al. (2018): DNA hypermethylation-mediated downregulation of antioxidant genes contributes to the early onset of cataracts in highly myopic eyes. Redox Biol 19: 179-189.
36. Zhang D, Li J, Lu T, et al. (2024): Illuminating shared genetic associations between oesophageal carcinoma and pulmonary carcinoma risk. J Cancer 15: 2412-2423.
37. Li D, Liang J, Guo W, et al. (2022): Integrative analysis of DNA methylation and gene expression data for the diagnosis and underlying mechanism of Parkinson's disease. Front Aging Neurosci 14: 971528.
38. Song B, Qiu Y, Wang Z, et al. (2025): The causal relationship between gut microbiomes, inflammatory mediators, and traumatic brain injury in Europeans: evidence from genetic correlation and functional mapping annotation analyses. Biomedicines 13: 753.
39. Feng P, Li Z, Li Y, et al. (2022): Characterization of different subtypes of immune cell infiltration in glioblastoma to aid immunotherapy. Front Immunol 13: 799509.
40. Chriett S, Lindqvist A, Shcherbina L, et al. (2021): SCRT1 is a novel beta cell transcription factor with insulin regulatory properties. Mol Cell Endocrinol 521: 111107.
41. Wan XM, Zheng C, Zhou XL (2022): Puerarin prevents cadmium-induced mitochondrial fission in AML-12 cells via Sirt1-dependent pathway. Ecotoxicol Environ Saf 248: 114302.
42. Xu G, Zhang J, Shao C, et al. (2025): Puerarin alleviates cerebral ischemia/reperfusion (CIR)-induced neurocyte oxidative stress and apoptosis via DNA demethylation-mediated PI3K/Akt activation. Phytomedicine 145: 157094.
43. Sheng G, Wu Y, Liu H, et al. Puerarin improves cancer-induced bone pain by recovering mitochondrial dysfunction in the spinal cord. J Neuroimmune Pharmacol 20: 67.
44. Qi D, Lu Y, Qu H, et al. (2025): CLDN6 triggers NRF2-mediated ferroptosis through recruiting DLG1/PBK complex in breast cancer. Cell Death Dis 16: 122.
45. Hu S, Yao Y, Wei ZY, et al. (2022): Deletion of p38γ attenuates ethanol consumption- and acetaminophen-induced liver injury in mice through promoting Dlg1. Acta Pharmacol Sin 43: 1733-1748.